Energy Flow Analysis of Vocal Fold Models

Scott L. Thomson[*]*, Luc Mongeau, & Steven H. Frankel*

School of Mechanical Engineering
Purdue University, West Lafayette, Indiana, USA
[*]Current affiliation: Brigham Young University, Department of Mechanical Engineering, Provo, Utah, USA
thomson@byu.edu; mongeau@ecn.purdue.edu; frankel@ecn.purdue.edu

Abstract

Complementary physical and computational models were developed and studied in order to investigate the aerodynamic energy transfer mechanisms that facilitate self-sustained vocal fold vibration. The physical model was fabricated using a flexible polyurethane compound. The model size, shape, and material properties were generally similar to corresponding human vocal fold characteristics. The numerical model was developed using geometry, boundary conditions, and material properties similar to those of the physical model. Analysis of the numerical results support the hypothesis that a cyclic variation of the orifice profile from a convergent to a divergent shape leads to a temporal asymmetry in the average wall pressure, which is the key factor for the achievement of self-sustained vocal fold oscillations.

1. Introduction

The primary mechanism of vocal fold vibration is a coupling between the air pressure and the tissue motion. It has been shown [1] that the average intraglottal pressure must be greater during the opening phase than during the closing phase in order for there to be a positive net transfer of energy from the airflow to the vocal folds; a positive value is required to overcome damping within the vocal fold tissue. It has been postulated [1] that one likely contributor to this pressure asymmetry is the converging-diverging motion of the medial surface of the vocal folds.

The hypothesis that a cyclic converging/diverging orifice profile is needed for self-sustained vocal fold oscillations to be maintained was verified using complementary experimental and numerical methods. The numerical model provided quantitiative flow data that could not be conveniently measured using physical experiments.

2. Theory

The kinetic energy balance for a control volume comprised of a fluid region is [2, 3]:

$$\underbrace{\frac{d}{dt}\int_V E\,dV}_{\text{I}} = \underbrace{\int_{S_i,S_e} E u_i(-n_i)\,dS}_{\text{II}} - \underbrace{\int_S u_i \tau_{ij}(-n_j)\,dS}_{\text{III}} - \underbrace{\int_V \phi\,dV}_{\text{IV}} \quad (1)$$

where E is the kinetic energy per unit volume, V is the control volume of interest, u is the fluid velocity, S is the control surface (S_i and S_e denote the inlet and exit surfaces, respectively), n is the unit vector normal to the control surface, τ_{ij} is the fluid stress tensor, and ϕ is the viscous dissipation term. Note that the influences of gravity and compressibility have been neglected in (1). The terms in (1) have the following physical significance [2, 4]:

- I: Rate of change of kinetic energy within the control volume.
- II: Rate of transport of kinetic energy out of the control volume through inlet and exit surfaces. This term is zero along impermeable surfaces.
- III: Rate of work done by fluid stress on the surroundings. This term is evaluated over the entire control volume surface. Normal and viscous forces are included in the stress term, τ_{ij}.
- IV: Rate of kinetic energy dissipation due to fluid viscosity.

Since the terms in (1) denote rates of energy transfer, or energy "flow," they have units of power (J/s). The energy transfer during a certain time period is calculated by integrating the terms in (1) over a specified time interval.

Term III evaluated along the vocal fold surface represents the energy flow from the air stream to the solid tissue, and is the focus of the analysis presented below.

3. Physical and Numerical Models

3.1. Physical Model

An artificial vocal fold model was fabricated using a flexible polyurethane compound, cast into an idealized shape of the vocal folds. The shape, shown in Fig. 1, was patterned after that used by Scherer et al. [5]. The length scale was the same as that of the human vocal folds. The Young's modulus of the material was approximately 14 kPa. The model oscillated at a frequency of approximately 120 Hz, with an onset pressure of approximately 1.2 kPa. Details of the physical model construction, experimental setup, and behavior can be found in [3].

3.2. Numerical Model

The finite element method was used to simulate the motion of the physical vocal fold model. The commercial code ADINA (ADINA R&D, Inc., Boston, Massachusetts), which is designed for analyzing coupled fluid-structure systems, was used. The computational domain is shown in Fig. 1. The model size, shape, and material properties were defined based on the physical model. The structural domain was two-dimensional and allowed for large deformation and large strain by using a hyperelastic material model. The fluid domain (air) was two-dimensional, laminar, and incompressible, and was governed by the Navier-Stokes equations; this allowed for flow separation and unsteady effects to be included. The solid and fluid domains were fully coupled. A fluctuating pressure, p_s, was imposed along the inlet (AC). The magnitude of p_s, taken from experimental data, varied sinusoidally about a

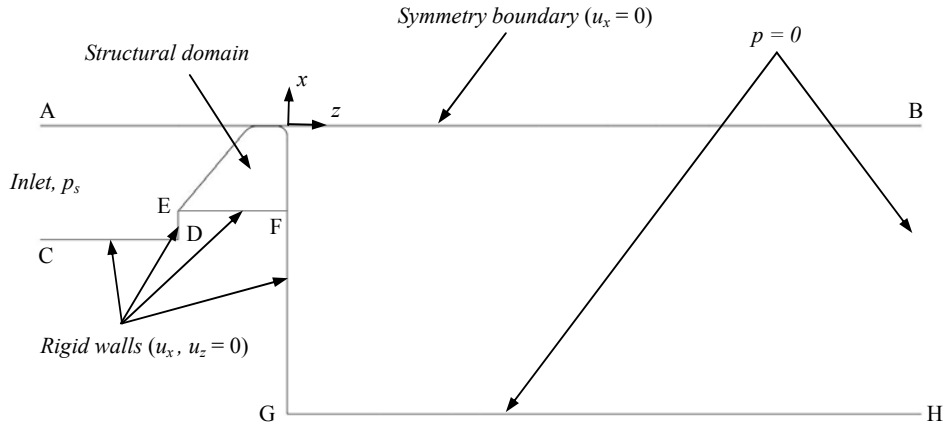

Figure 1: *Outline of the numerical domain. The outlet along BH was located further downstream than what is shown.*

mean value of 2 kPa with an amplitude of 1.2 kPa. Further details are found in [3].

4. Numerical Results and Discussion

Figure 2 shows the position of the solid domain surface over one oscillation period. The medial surface profile was alternately convergent-divergent. The significant inferior-superior motion was a result of the solid domain having been defined using a homogeneous, isotropic material (as opposed to the multi-layer, anisotropic structure of the human vocal folds).

Figure 3a shows the orifice width over one cycle. Also shown in Fig. 3a is the "subglottal" pressure, p_s, that was applied at the fluid domain inlet. The orifice width varied from approximately 0.2 mm at the time of minimum opening to 2.8 mm at the maximum opening. Note that the orifice width refers to the full orifice width (twice the distance between the point on the medial surface of the solid domain closest to the plane of symmetry in the fluid domain). The local maximum at approximately t = 0.058 s coincided with the time during which the orifice was transitioning from a convergent to a divergent shape.

Figure 3b is discussed separately below. Figure 3c shows the rate of energy transfer to the solid domain over one period due to the total fluid stress; this quantity is equivalent to Term III in Eq. (1) evaluated along the solid domain surface. Also shown are the individual contributions of the pressure and viscous stresses; the contribution of the viscous stresses was everywhere negligible, and the total energy transfer was nearly entirely due to the normal pressure. The maximum contribution of the viscous stresses reached only about 1% of the maximum energy flow.

The net area under the curve over one cycle in Fig. 3c is positive; approximately twice as much energy was imparted to the solid domain than what was recovered. The remainder was dissipated in the solid due to viscous damping.

Figures 4 through 6 show the wall position, the normal component of velocity, the wall pressure distribution, and the energy flow intensity (Term III) at three different times. At time t = 0.0551 s (Fig. 4), the orifice was nearly closed, and the profile was slightly divergent and transitioning to a convergent shape. The inlet pressure was approaching its maximum specified value. The net energy flow to the

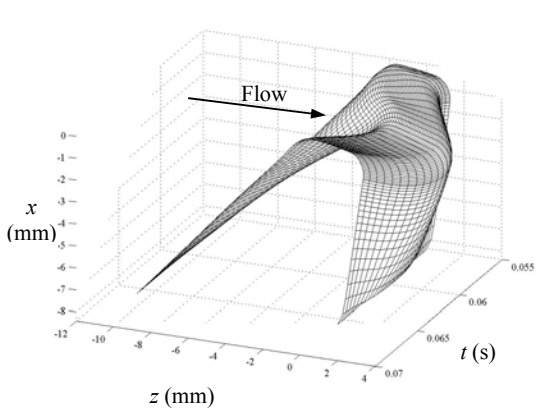

Figure 2: *Numerical model surface position.*

structure was zero. At the time of maximum energy flow to the structure (t = 0.0570 s; Fig. 5), the pressure was in phase with the surface velocity over most of the surface; thus the energy flow was distributed along nearly the entire length of the inferior and medial surfaces. The orifice profile was convergent and the medial surface was slightly concave. At the time of maximum energy flow from the solid to the flow (t = 0.0642 s; Fig. 6), the orifice profile was divergent and the orifice was closing. The energy flow was negative since the velocity and pressure terms were out of phase. The region of greatest energy transfer was near the medial, inferior tip (compare Figs. 6a and 6c).

Figure 3b shows the spatially averaged pressure, p_{avg}, where p_{avg} is defined as

$$p_{avg} = \frac{1}{L}\int p dl \,, \tag{2}$$

where L is the length of the vocal fold surface. It can be seen from Fig. 3b that the average pressure was never negative. The time-averaged pressure, p_{mean}, during positive energy flow to the solid (orifice opening) was greater (p_{mean} = 1.3 kPa) than that during negative energy flow (orifice closing; p_{mean} = 0.72 kPa). This is in agreement with the observation by Titze [1] that for self-sustained oscillations to be achieved, the net

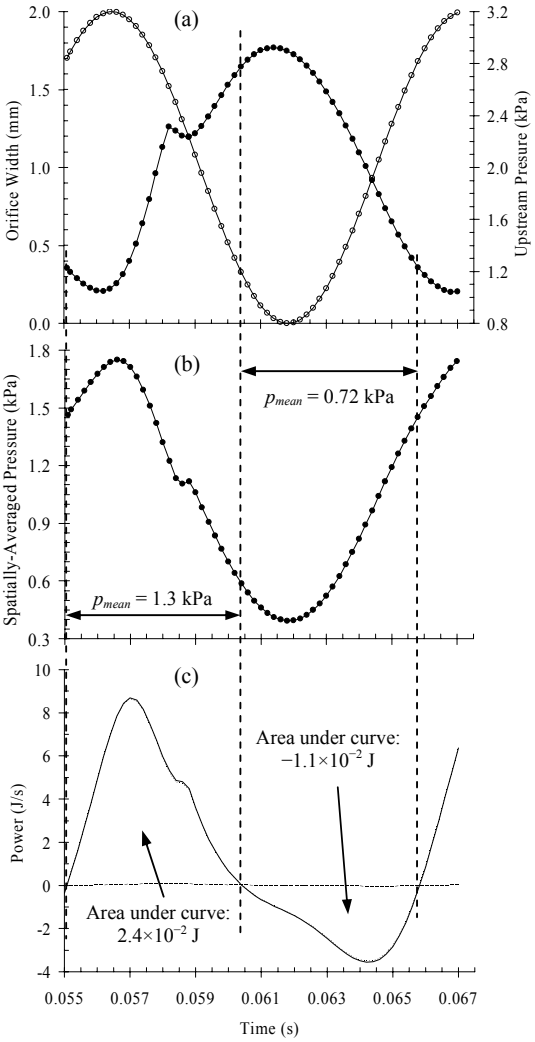

Figure 3: *(a) –●–: Orifice width; –○–: Upstream pressure; (b) Spatially-averaged surface pressure; (c) Net rate of energy transfer to the surface due to total, pressure, and viscous stresses.* ——: $u_i\tau_{ij}(-n_j)$; · · ·: pu_in_i; – – –: $u_i\tau_{ij}(-n_j) - pu_in_i$.

intraglottal pressure during closing must be either negative or "less positive" than the net intraglottal pressure during opening.

In further agreement with Titze's theory, a comparison between Figs. 5 and 6 shows that the energy flow to the structure is assisted by the medial surface convergent-divergent motion. When the profile was convergent (Fig. 5), the flow was attached and the magnitude of the pressure was significant over the entire medial surface of the solid (Fig. 5b). The energy flow was thus also significant over the medial surface of the solid (Fig. 5c). When the profile was divergent (Fig. 6), the flow separated from the medial surface, causing the pressure to be nearly zero along a significant portion of the medial surface (Fig. 6b). This resulted in the energy flow being confined to a smaller region along the vocal fold surface (Fig. 6c). This temporal asymmetry in pressure distribution

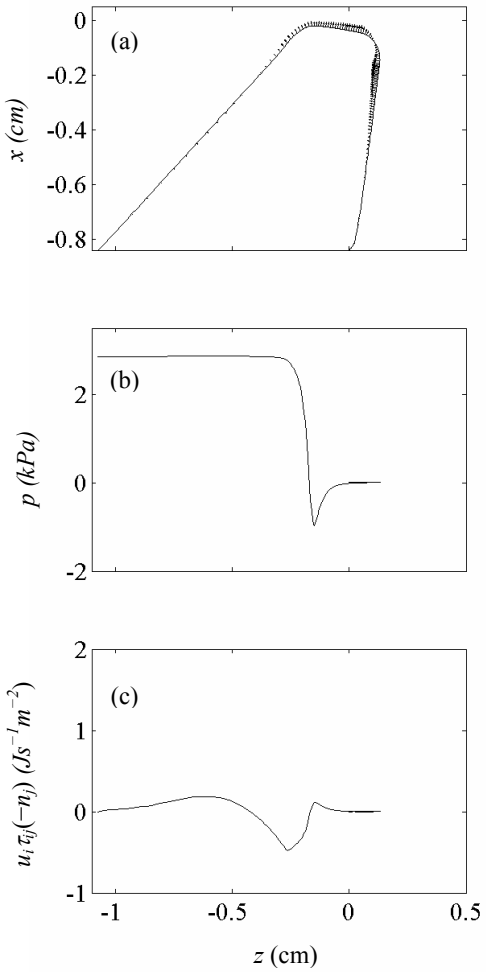

Figure 4: *Different quantities along the fold surface at time t = 0.0551 s. (a)* ——*: x vs. z;* → *: u_in_i vs. z; (b) p vs. z; (c) $u_i\tau_{ij}(-n_j)$ vs. z.*

caused a similar temporal asymmetry in the energy flow, allowing for oscillations to be achieved.

5. Conclusions

Numerical simulations of a continuum vocal fold model were used to calculate the energy transferred from the fluid domain to the structural domain during one period of regular oscillations. It was shown that the aerodynamic viscous effects only minimally contributed to the overall energy transfer. It was further shown that the alternating convergent-divergent orifice profile resulted in a greater net pressure within the orifice during orifice opening than during orifice closing. This temporal asymmetry in net orifice pressure caused a temporal asymmetry in the energy flow to the solid domain, which allowed for oscillations to be maintained. The results support the hypothesis that a cyclic variation of the orifice profile from a convergent to a divergent shape leads to a temporal asymmetry in the average wall pressure, which is the key factor for self-sustained oscillations of the vocal folds to be achieved.

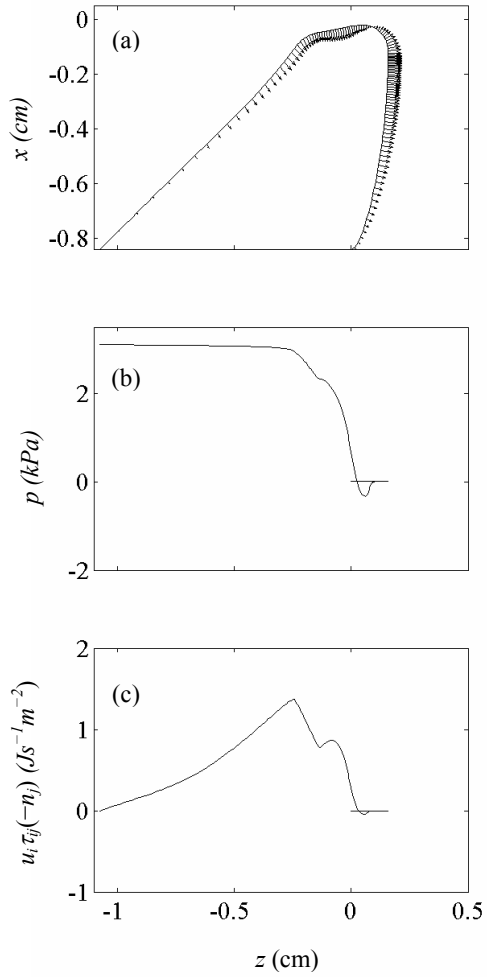

Figure 5: *Different quantities along the fold surface at time t = 0.057 s. (a) ——: x vs. z; → : u_in_i vs. z; (b) p vs. z; (c) $u_i\tau_{ij}(-n_j)$ vs. z.*

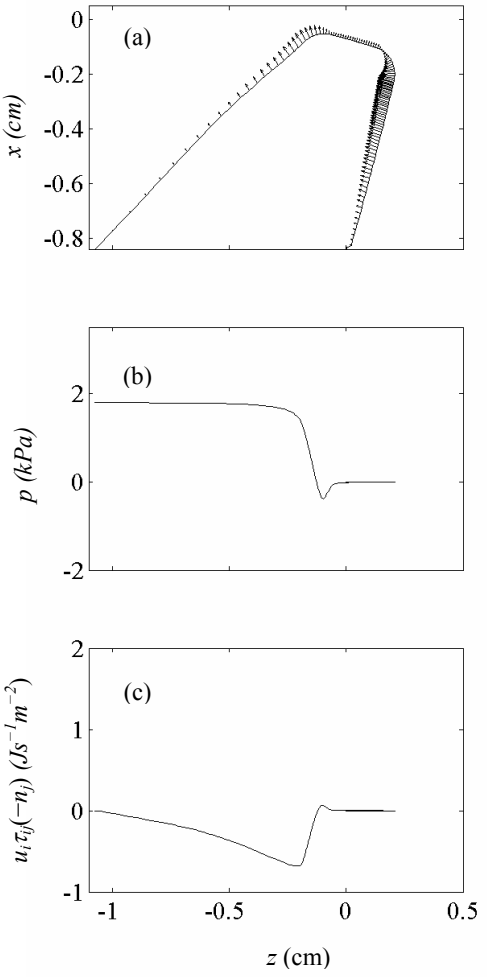

Figure 6: *Different quantities along the fold surface at time t = 0.0642 s. (a) ——: x vs. z; → : u_in_i vs. z; (b) p vs. z; (c) $u_i\tau_{ij}(-n_j)$ vs. z.*

6. References

[1] Titze, I.R., 1988. The physics of small-amplitude oscillation of the vocal folds. *J. Acoust. Soc. Am.* 83, 1536-1552.

[2] Kundu, P.K., 1990. *Fluid Mechanics.* Academic Press, San Diego, California.

[3] Thomson, S.L., 2004. *Fluid-Structure Interactions Within the Human Larynx*. Ph.D. Disseration, Purdue University, West Lafayette, Indiana.

[4] Slattery, J.C., 1972. *Momentum, Energy, and Mass Transfer in Continua*. McGraw-Hill, Inc.

[5] Scherer, R.C.; Shinwari, D.; De Witt, K.J.; Zhang, C.; Kucinschi B.R.; Afjeh, A.A., 2001. Intraglottal pressure profiles for a symmetric and oblique glottis with a divergence angle of 10 degrees. *J. Acoust. Soc. Am.* 109, 1616-1630.